



AIAA-2003-0754

**Recent Enhancements to the National
Transonic Facility (Invited)**

W.A. Kilgore, S. Balakrishna, C.W. Bobbitt and P. Underwood
NASA Langley Research Center
Hampton, Virginia

41st AIAA Aerospace Sciences Meeting & Exhibit
6-9 January 2003
Reno, Nevada



RECENT ENHANCEMENTS TO THE NATIONAL TRANSONIC FACILITY

W. A. Kilgore*, S. Balakrishna†, C. W. Bobbitt‡ and P. Underwood§
Aerodynamics, Aerothermodynamics, and Acoustics Competency
NASA Langley Research Center
Hampton, Virginia

ABSTRACT

The National Transonic Facility continues to make enhancements to provide quality data in a safe, efficient and cost effective method for aerodynamic ground testing. Recent enhancements discussed in this paper include the restoration of reliability and improved performance of the heat exchanger systems resulting in the expansion of the NTF air operations envelope. Additionally, results are presented from a continued effort to reduce model dynamics through the use of a new stiffer balance and sting.

INTRODUCTION

The National Transonic Facility (NTF) located at the NASA Langley Research Center is a closed circuit continuous flow wind tunnel used to obtain aerodynamic data at subsonic and transonic speeds up through full-scale Reynolds numbers for most flight vehicles. The NTF can operate as a conventional pressure wind tunnel using dry air as the test medium and a cooling coil for temperature control or as a cryogenic pressure tunnel using nitrogen as the test medium and evaporating liquid nitrogen into the flow to control temperature.

The NTF test section is a square filleted cross-section (approximately 8.2 feet per side) that can be configured either with slotted-walls (6% open ratio) or solid walls. It can operate at Mach numbers from 0.1 up to 1.2 (1.1 in air), Reynolds numbers up to 146 million per foot, total temperatures from 140°F down to -260°F, and total pressures from atmospheric up to 130 psia. The NTF has a 101MW fan drive system that provides the necessary power to drive the test gas

around the circuit with dynamic pressures up to 7000 psf. Figures 1 and 2 show the standard operational envelopes for cryogenic nitrogen operations at -250°F and air operations at 120°F, respectively. Both sting-mounted full-span models and wall-mounted semi-span models can be tested in the facility.

NTF AIR OPERATIONS IMPROVEMENTS

For air operations, the NTF operates as a conventional tunnel with the added benefits of the ability to pressurize and the ability to maintain temperature. Operating the NTF in air mode provides a cost effective method of testing while still achieving higher Reynolds number testing than many other ground-based test facilities.

The air operations envelope is shown in figure 2. The NTF cannot run below atmospheric pressures ($P_T \geq 14.7$ psia) and therefore the air envelope has a minimum Reynolds number limit for all Mach numbers. For low-speed testing ($M < 0.5$), the maximum Reynolds number is limited by the maximum allowed tunnel total pressure ($P_T = 130$ psia). For supersonic testing, the limit is a Mach number of 1.1 set by the test-section geometry. For transonic testing, the maximum Reynolds number is limited by the capacity of the cooling coil to remove sufficient heat to hold the free stream total temperature constant.¹

As its name suggests, the National Transonic Facility spends much of its time operating in the transonic regime. Therefore, the limitation imposed by the capacity of the cooling coil is of great importance to the facility. Degradation of this system over time has reduced its capacity and therefore, further limited the transonic air operations envelope. An additional problem with the cooling coil has been leaks, which have introduced moisture into the tunnel, requiring increased expense to dry the tunnel. Furthermore, at times this moisture in the tunnel has compromised test data by forming frost on the test article.

* Facility Manager - National Transonic Facility, NASA-LaRC, Senior Member, AIAA

† Senior Research Scientist, ViGYAN Inc.

‡ Research Engineer, NASA-LaRC

§ Test Engineer, ViGYAN Inc., Member, AIAA

This material is declared a work of the U. S. Government and is not subject to copyright protection in the United States.

To combat these problems while still maintaining the NTF's cost effective air operations, work was recently performed to restore the integrity of this cooling coil and to increase the capacity of the cooling system thereby expanding the transonic air operations envelope. Details of this work, as well as the results and future plans, are described below.

Cooling System Background

The purpose of the NTF cooling system is to balance the heat entering and exiting the tunnel circuit such that the desired testing temperature is stable. The majority of the heat introduced into the tunnel circuit is through the fan drive system (with a maximum power of 101MW). For tunnel operations using nitrogen as the test medium, liquid nitrogen is evaporated into the tunnel circuit between the diffuser and fan to achieve the desired stable temperature. For air operations, the centerpiece of the cooling system is the cooling coil, which is a cross-flow type heat exchanger located in the settling chamber of the tunnel.

Figure 3 represents this type of cross flow heat exchanger where the cooling water flows through the cooling coil tubes and removes heat from the dry air cross flow.

Cross-flow heat exchangers operate according to the following heat transfer rate equation:

$$q = U A F \Delta T_{lm} \tag{1}$$

where

q = heat transfer rate

U = overall heat transfer rate coefficient

A = effective surface area for heat exchange

F = correction factor for cross-flow heat exchanger (function of heat exchanger design and inlet and exit temperatures of the two fluids, range 1.0 for ideal down to 0.5)

$$\Delta T_{lm} = (\Delta T_2 - \Delta T_1) / \ln (\Delta T_2 / \Delta T_1)$$

= logarithmic mean temperature difference

$$\Delta T_1 = T_{air,in} - T_{water,out}$$

$$\Delta T_2 = T_{air,out} - T_{water,in}$$

Based on this equation the heat transfer rate, q, (from the point of view of the heat exchanger system) is controlled by the cooling coil design, size, physical condition, and the inlet and exit flow temperatures of the cooling water and dry air.

Figure 4 shows a piping schematic of the NTF cooling system. The cooling coil, located in the tunnel settling chamber, consists of two layers (upstream and downstream) of 781 finned (8 fins/inch) elliptical copper tubes (inside dimensions of 1.3 inches x 0.43 inches) arranged in four staggered rows that extend across the settling chamber (Figure 5). Each layer has 18 bundles of which 6 bundles are 36 inches wide and 12 bundles are 18 inches wide with the lengths ranging from 20 to 36 feet. The upstream layer has water flowing from the bottom to the top, and the downstream layer has water flowing from the top to the bottom. The total effective surface area, A, for the cooling coil is approximately 105,500 ft².

The water supplied to the cooling coil inlet comes from a 78,000 gallon cooling tower water sump. This supply water is pumped via two large water pumps to the cooling coil through a long supply pipe (341 feet of 16 inch diameter carbon steel pipe followed by 120 feet of 10 inch stainless steel pipe) at a constant flow rate of about 8600 gallons per minute (gpm). At the end of the supply pipe the water is distributed into a 10 inch diameter manifold that feeds 36 smaller pipes (2 inch, 3 inch and 4 inch) leading to each bundle. As the water passes through the cooling coil it increases in temperature as it absorbs the heat of the tunnel circuit flow. The warm return water is then returned to the cooling tower through 36 smaller pipes into a 10 inch diameter manifold and then enters the long return pipe (137 feet of 10 inch stainless steel pipe followed by 299 feet of 16 inch diameter carbon steel pipe). Prior to reaching the cooling tower the water passes through a bypass valve where it is either passed back into the water supply pipe or continues on and is dropped into the top of the cooling tower. The amount of water through the bypass valve is based on the desired tunnel total temperature. As the return water is dropped into the top of the cooling tower it passes through spray nozzles and mixing screens to cool the water. Additional cooling is provided by three forced draught fans located at the top of the cooling tower that mix atmospheric air through the tower for atomized spray cooling of the water thereby exchanging heat with the ambient air. Ideally, with this method the water can be cooled to the atmospheric dew point temperature. The

thermal capacity of the cooling tower is therefore dictated by the difference between outlet water temperature and ambient atmospheric dew point. Assuming an average summer day in Hampton, Virginia, the ideal capacity of the tower is about 50MW with a seasonal variation of ± 3 MW.

For a given tunnel condition, the outlet water temperature from the cooling coil is affected by the inlet temperature and the mass flow of water through the system. As the mass flow increases, the outlet temperature decreases but the heat transfer rate and efficiency of the heat exchanger increases. Therefore, for a given heat exchanger geometry and minimum inlet water temperature available (set by the cooling tower), an increase in mass flow is the only way to increase the capacity of heat removal of the cooling coil. Currently, the thought is to increase the mass flow rate of the system to increase the capacity of the cooling system (thereby increasing the transonic air test envelope), which will be discussed later.

An additional aspect of the NTF cooling system for air operations is the fact that the cooling coil must be drained and dried prior to the commencement of cryogenic operations. This process is necessary to prevent any water from remaining in the tubes, which could freeze, expand, and burst the tubing.

Operation and Deterioration

After several years of operation, there were indications that the capacity and integrity of the NTF cooling system was degrading. One indication was the reduction in heat transfer rate from the designed 34MW limit in 1984 down to 27MW in 1999. The second was the increased number of incidents of cooling coil tube ruptures during the cycling between warm and cryogenic operations.²

Both of these symptoms pointed toward the restriction of flow through the cooling coil tubes, and if some tubes were completely blocked, the effective surface area for heat transfer would be reduced. From the equation for heat transfer rate for this cross-flow heat exchanger (Equation 1), it can be seen that either of these situations would result in a reduction of heat transfer capability. Rupturing of tubes is an indication that water is still trapped in the tubes after the cooling coil draining and drying processes are complete. This trapped water then freezes, expands, and ruptures the tube. An example of a rupture is shown in figure 6. The only way this water could be trapped in the

tubes is if some debris were present to prevent it from being removed.

While the reduction of the heat transfer capability was troubling, the rupturing of the tubes was devastating. While procedures existed for detecting leaks prior to the refilling of the cooling coil after cryogenic operations, it was still possible for some small leaks to escape notice, or for weakened tubes to rupture after the cooling coil had been refilled. As a result, water would be introduced into the tunnel. If even small amounts of this water remained in the tunnel during cryogenic operations, it would be possible for frost to form on the test article (shown in figure 7) that could compromise the aerodynamic data quality.

More and more time and money were being spent to dry the tunnel, to recover from ruptures and to minimize the potential for frost until eventually the decision was made to remove the cooling coil from service. It was felt that the major contribution of the NTF was high Reynolds number cryogenic testing, and that this capability should not be compromised by risks associated with air operations. Therefore, in October 2001 the NTF cooling coil was removed from service and air operations were stopped.

Evaluation/Repair/Return to Air Operations

While it was and is true that the major contribution of the NTF is the high Reynolds number data it provides, it soon became clear that the operation of the NTF as a conventional pressurized air tunnel was itself a valuable asset. Therefore, a team was formed to evaluate, repair, and return the cooling coil to reliable operational status.

The team's first job was to determine the causes of the problems and the extent of these problems. Figure 8 shows the relative blockage of each cooling coil bundle as determined by high pressure air purges of the system. It can be seen that many of the bundles, indicated by the darker colors, (particularly bundle 9) had restricted flow. Analysis of the cooling system revealed that the main contributor to the blockage was rust coming from the carbon steel piping in the system.

Once these blocked bundles were identified, the clogged or leaking tubes were either repaired or replaced. After this repair, internal and external pneumatic pressure leak checks were performed on the system. When leaks were found, they were repaired and rechecked until it was clear that all leaks were eliminated. Then leak checks were

performed using pressurized argon gas (for detecting small leaks) and internal vacuum checks to completely verify the cooling coil integrity. After successfully completing these leak checks the system was flushed with high pressure air and then with water to remove any remaining debris. After this, a hydrostatic test was performed to ensure the cooling coil integrity.

Beyond this effort of repair, it was also desired to prevent this situation from reoccurring, and to give early warning if a problem did develop. To address these issues, the team instituted several changes. To prevent further contamination of the cooling coil, some of the deteriorated carbon steel piping was replaced with stainless and a strainer was installed on the water supply side to prevent large debris from reaching the cooling coil. Figure 9 shows some of the debris captured by the strainer. For detection of problems additional moisture monitoring instrumentation was installed in the tunnel circuit to indicate a possible leak in the cooling coil.

Furthermore, procedures and processes were modified to minimize the possibility of future moisture contamination to the tunnel circuit. The modifications to the process of drying the cooling coil prior to cryogenic operations now includes the use of a vacuum pump attached to the cooling coil. The purpose of the vacuum pump is to lower the pressure inside the cooling coil to 0.2 psia to "boil off" any remaining water (boiling point is -70°F at 0.2 psia). To accelerate this process the tunnel is heated to above 100°F . The vacuum pump also provides an additional leak check of the cooling coil prior to refilling it with water.

Results

The results from this effort can be seen in two ways. First, since re-entry into operation (October 2001), the cooling coil has not experienced any incidents of leaks. Second, the cooling coil repair has restored the cooling capacity of the system. Figure 10 is a plot of the log mean temperature difference, ΔT_{lm} (see equation 1), versus tunnel fan power and shows graphically the increase in cooling coil performance from before to after the repairs. From the equation for the heat exchange rate, it can be seen that for a given ΔT_{lm} the fan power removed has increased. This change can be attributed to an increase in efficiency (seen in an increase in the correction factor F), and/or to a decrease in the thermal resistance (increase in U) and a restoration in the effective cooling area of the coil (increase in A). Changes to all of these

parameters would be expected from cleaning the cooling coil and repairing/replacing sections of blocked tubes. Figure 10 shows the new maximum capacity of the cooling system to be near 45MW, while as stated earlier the design capacity of the system was only 34MW. This difference can be attributed to the fact that the cooling system is capable of lower inlet water temperatures and higher outlet water temperatures than were actually assumed in the original design.

High Power Conditions

The repairs to the cooling coil restored the integrity of the system and increased in the capacity to approximately 45MW. The current Reynolds number limits of the transonic air operations envelope available for NTF were recently operationally confirmed. For this test, a Mach number was set, and the tunnel pressure increased until the maximum Reynolds number was reached where the cooling system could still maintain a constant temperature. This process was repeated for a range of Mach numbers. The results of this test are shown in Table 1. It should be noted that this test was run in February 2002 and a constant tunnel temperature of 130°F was allowed, both of which result in some increase in the cooling capacity of the system beyond 45MW.

Table 1 - Sustained Operations Conditions

M	P_T (psia)	T_T ($^{\circ}\text{F}$)	ΔT ($^{\circ}\text{F}$)	P_{max} (MW)	Re/ft (millions)
0.700	61.00	126.6	± 0.2	48.0	13.27
0.840	42.01	126.9	± 0.3	49.3	10.87
0.870	37.03	130.0	± 0.3	46.3	9.66
0.910	35.95	130.0	± 0.7	48.4	9.55

Test programs at the NTF have already exploited this expanded test envelope. Figure 11 shows the additional test conditions obtained in air for two test programs that were run both before and after the improvements to the NTF cooling system.

It is desired to increase the heat removal capacity of the cooling coil to further extend the transonic air operations envelope. An approach to increasing the operational envelope is "pulse" testing. For this method of testing, the cooling capacity is exceeded briefly (about 10 minutes) while data is being obtained at a desired condition. Since the cooling capacity is exceeded, the temperature is always climbing; however, this change in temperature does not exceed acceptable tolerance limits for the short duration of

the run. Table 2 shows the results of one pulse test where an alpha sweep was run at $M=0.84$ with a fan power of almost 60MW. For this alpha sweep, the temperature only varied a total of 3°F.

Table 2 - Pulse Operations Conditions

M	P_T (psia)	T_T (°F)	ΔT (°F)	P_{max} (MW)	Re/ft (millions)
0.840	51.98	133.1	± 1.4	59.2	13.27

As stated earlier, another method of further extending this test envelope is to increase the mass flow of cooling water through the cooling coil. Figure 10 shows the experimental verification of this for the NTF system by comparing a 5600 gpm flow rate (one pump operating, Pump 3 – see figure 10) versus 8600 gpm (both pumps operating, Pumps 3 & 4).

The mass flow for the NTF system could be increased either by increasing the pump pressure or by reducing losses in the system. Losses in the system could be reduced by straightening and shortening pipe lengths and/or increasing pipe diameters. The cooling coil team study shows that the total length of the 16 inch diameter carbon steel piping (640 feet) could be reduced by about 150 feet, and many bends and elbows could be removed. Additionally, the study shows that the 16 inch carbon steel pipe continues to deteriorate posing serious danger to the future of the cooling system and must be replaced. This piping change would result in an estimated increase in mass flow rate of about 700 gpm (from 8600 to 9300).³ Work is currently underway to replace this last section of carbon steel pipe.

Using the analysis for a cross-flow heat exchanger presented in figure 10 it is possible to predict the new cooling coil capacity with 9300 gpm water flow. Two gradients can be defined under equilibrium conditions that characterize the cooling coil. The first is fan power/ ΔT_m , which is about 1.1 MW/°F. The second is based on the maximum recorded ΔT_m of 42.5°F at a flow rate of 8600 gpm. This provides a second characteristic of 202 gpm/°F. As shown in figure 10 the 9300 gpm will increase to the ΔT_m from 42.5 to 46°F corresponding to new maximum of 51MW.

Based on the cooling tower it appears that 50MW is the practical limit for the current systems since increases beyond this would require a change to

the cooling tower, as its average capacity is 50MW.

DYNAMICS

Throughout the history of high Reynolds number testing at the NTF several test programs were severely limited or cut short because of dynamics. These test limitations manifest themselves as excessive balance dynamic loads, model displacements and increased data scatter. An extensive effort was undertaken at the facility that provided significant reductions of the tunnel structural dynamics and a small reduction in model dynamics.⁴ Despite these reductions the limitations still exist as testing programs continue to desire higher loads and higher angles of attack. In an effort to overcome these limitations a new balance (NTF-116A) and new upper swept sting were developed to obtain higher loads and provide increased stiffness as compared with the NTF-113 series balance and upper swept sting combination previously used.⁵

113 Balances

The 113 balances are the workhorse balances at the NTF and have provided years of reliability and quality data. The 113 balance, shown in the top of figure 12, is made of a single piece of high strength maraging steel and has a cylindrical cross section that is 2.375 inches in diameter and 15.565 inches long. The metric end has a precision ground cylinder that is secured to the model with an interference fit dowel pin. The non-metric end has a precision ground cylindrical taper fit with a key and set screw flats for securing to the sting.

Each balance has two complete and independent sets of temperature compensated strain gage bridges for measurement of six components (normal force, axial force, side force, pitching moment, rolling moment and yawing moment). A 113 balance is referred to as a "moment balance" because the normal force (NF), pitching moment (PM), side force (SF) and yawing moment (YM) are determined from individual bridge signals as shown below:

$$\begin{aligned} NF &= N1 + N2 \\ PM &= N1 - N2 \\ SF &= S1 + S2 \\ YM &= S1 - S2 \end{aligned}$$

116A Balance

In the development of the 116A several changes from the 113 balances were incorporated to achieve higher loads and increased stiffness. Like the 113 the 116A balance, shown in the bottom of figure 12, is made from a single piece of high strength maraging steel. The 116A has a larger cross section and is a non-symmetric octagonal shape 3.6 inches high and 4.0 inches wide. The larger octagonal shape provides greater load capability, and having the width greater than the height provides higher yaw directional stiffness. Again to increase stiffness, the length of 116A was reduced from the 113 by about two inches to 13.75 inches.

The 116A mechanical connections on both ends of the balance are flanges with through bolt connections. These flanges provide stiffer mechanical connections and have shorter interfaces allowing room for simple adaptors to provide proper placement of the balance within a model.

The 116A like the 113 has two complete and independent sets of temperature compensated strain gage bridges for measurement of six components. The 116A is referred to as a "force balance" because all forces and moments are direct outputs from the bridges. This configuration allows for an increase in the sensitivity of the strain measurement.

A direct comparison of the size, load capability and the accuracy of these two balances are presented in Tables 3, 4 and 5.

Table 3 – Balance Comparison

	NTF-113	NTF-116A
Material	Vascomax 200	Vascomax 200
Shape	cylindrical	octagonal
Diameter	2.375 in	3.6 in x 4.0 in
Length	15.575 in	13.75 in
Mounting, Metric	cylinder w/ dowel pin	flange w/ through bolts
Mounting, Non-Metric	cylindrical taper with key	flange w/ through bolts
Type	moment	force

Table 4 - Balance Load Capacity

Component	NTF-113B Full Scale	NTF-116A Full Scale
Normal Force (lb)	±6,520	±10,000
Axial Force (lb)	±400	±700
Side Force (lb)	±4,000	±4,000
Pitching Moment (in-lb)	±12,800	±40,000
Rolling Moment (in-lb)	±8,150	±16,000
Yawing Moment (in-lb)	±6,400	±24,000

Table 5 - Balance Accuracy

Component	113B Accuracy 95% Conf. (% of F. S.)	116A Accuracy 95% Conf. (% of F. S.)
Normal Force (lb)	0.05% (3.26 lb)	0.07% (7 lb)
Axial Force (lb)	0.24% (0.96 lb)	0.38% (2.66 lb)
Side Force (lb)	0.13% (5.2 lb)	0.05% (2 lb)
Pitching Moment (in-lb)	0.09% (11.5 in-lb)	0.11% (44 in-lb)
Rolling Moment (in-lb)	0.21% (17.1 in-lb)	0.2% (32 in-lb)
Yawing Moment (in-lb)	0.16% (10.3 in-lb)	0.05% (12 in-lb)

The 116A clearly provides a significant increase in the load capability over the 113 balances while maintaining acceptable accuracy.

New Sting

The new flange style mountings of 116A required a new sting, so the opportunity to add stiffness to the new sting design was undertaken. The requirements for this new upper swept sting were to attach to the 116A balance, conform to aerodynamic requirements, and provide additional stiffness in an attempt to further reduce model

dynamics. Figure 13 shows this new sting with the balance interface flange exposed.

To match the 116A balance capacity the new sting design required an increased stiffness for the normal force direction and pitching moment. Slight increases to the width and length of the vertical blade section and an increase in the diameter of the aft end (where it connects to the tunnel stub sting) accomplished this. Significant dimensional changes could not be made without compromising the aerodynamic quality of the sting.

A series of balance/sting deflection tests were made to experimentally determine the increased stiffness of the new balance/sting combination. Table 6 shows the comparison of the measured balance/sting deflection coefficients for the 113B/sting and the new 116A balance with the new sting.

Table 6 - Balance/Sting Stiffness

Stiffness Coefficient	113B and Upper Sting	116A and New Upper Sting
K_{NF} (deg/lb)	3.1×10^{-4}	2.1×10^{-4}
K_{PM} (deg/lb)	6.92×10^{-5}	2.4×10^{-5}

This table shows that the new balance/sting combination provides an increase in the stiffness in the normal force direction and pitching moment. This increase stiffness corresponds to less deflection for a given load.

Testing Results

The NTF recently completed a series of tests that was made possible with the new 116A balance and the new upper swept sting. The first benefit of the new balance/sting was the increase in the sting divergence dynamic pressure limit from 2700 psf to 4350 psf allowing higher loaded test conditions. The testing exploited the high load capacity of the balance as shown in figure 14. A majority of the testing program greatly exceeded the pitching moment capability of the older 113 balance/sting combination.

In addition to obtaining higher loads, the model dynamics were reduced as a result of the increased stiffness. The model frequencies shifted from 22Hz for the 113 balance/sting up to 35Hz for the 116A balance sting as shown in figure 15. Unfortunately the full benefit of the increased stiffness in the reductions of the model dynamics were not achieved because the 35Hz

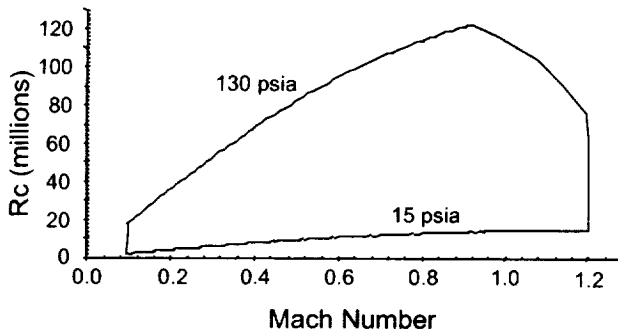
coincided with the tunnel structural frequency of the model support arc sector as shown in figure 16. With this increase in model frequency the model displacements were reduced and the test program was able to safely obtain 0.5° to 1.5° higher angles of attack.

SUMMARY

The National Transonic Facility continues to make enhancements to provide quality data in a safe, efficient and cost effective method for aerodynamic ground testing. Previous enhancements and studies at the NTF have focused on the nitrogen mode operations of the tunnel and air mode operations were seldom considered. The NTF is currently working on a focused effort to enhance its air mode operations through increased capability and improved efficiency. The enhancements of the cooling coil capacity from 34MW to 45MW and future enhancements presented in this paper highlight a portion of this ongoing effort. Additionally, the NTF has not lost focus on its primary mission to provide flight Reynolds number testing and therefore continues to make nitrogen operation improvements such as development of the NTF-116A balance and new upper swept sting. This new balance/sting combination has expanded the testing capability by providing higher testing loads with reduced model dynamics.

REFERENCES

1. Kilgore, W. Allen, and Balakrishna, S.: Control of Large Cryogenic Wind Tunnels, Study of the National Transonic Facility Controls, NASA Contractor Report 194977, September 1994
2. Bobbitt, C. W., and Everhart, J. L.: Status of the National Transonic Facility Characterization (Invited), AIAA Paper No. 2001-0755, January 2001
3. Butler, D. H., and Balakrishna, S.: NTF Cooling Coil Summary Report, NASA LaRC Contract NAS1-00135, Task 08RBJ, Subtask 3, June 2001
4. Kilgore, W. A., Balakrishna, S., and Butler, D.H.: Reduction of Tunnel Dynamics at the National Transonic Facility (Invited), AIAA Paper No. 2001-1162, January 2001
5. Parker, P. A.: Cryogenic Balance Technology at the National Transonic Facility (Invited), AIAA Paper No. 2001-0758, January 2001



$$Rc = (Re/ft) \cdot (0.1) \cdot (\text{test section area})^{0.5} = (Re/ft) \cdot (0.82)$$

Figure 1 - Cryogenic Nitrogen Operations Envelope (-250°F)

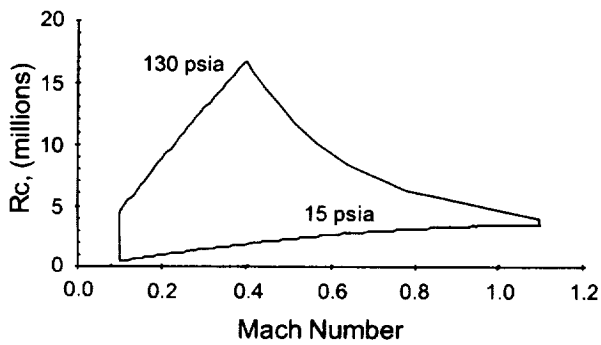


Figure 2 - Air Operations Envelope (120°F)

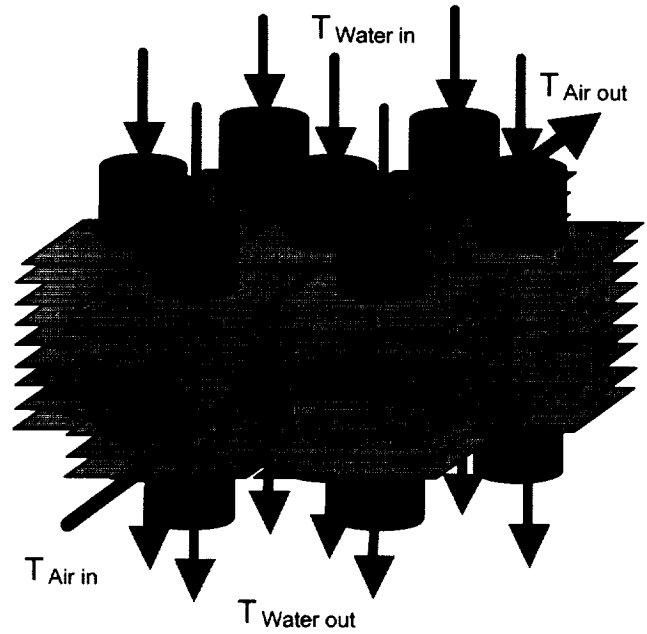


Figure 3 - Cross-Flow Type Heat Exchanger

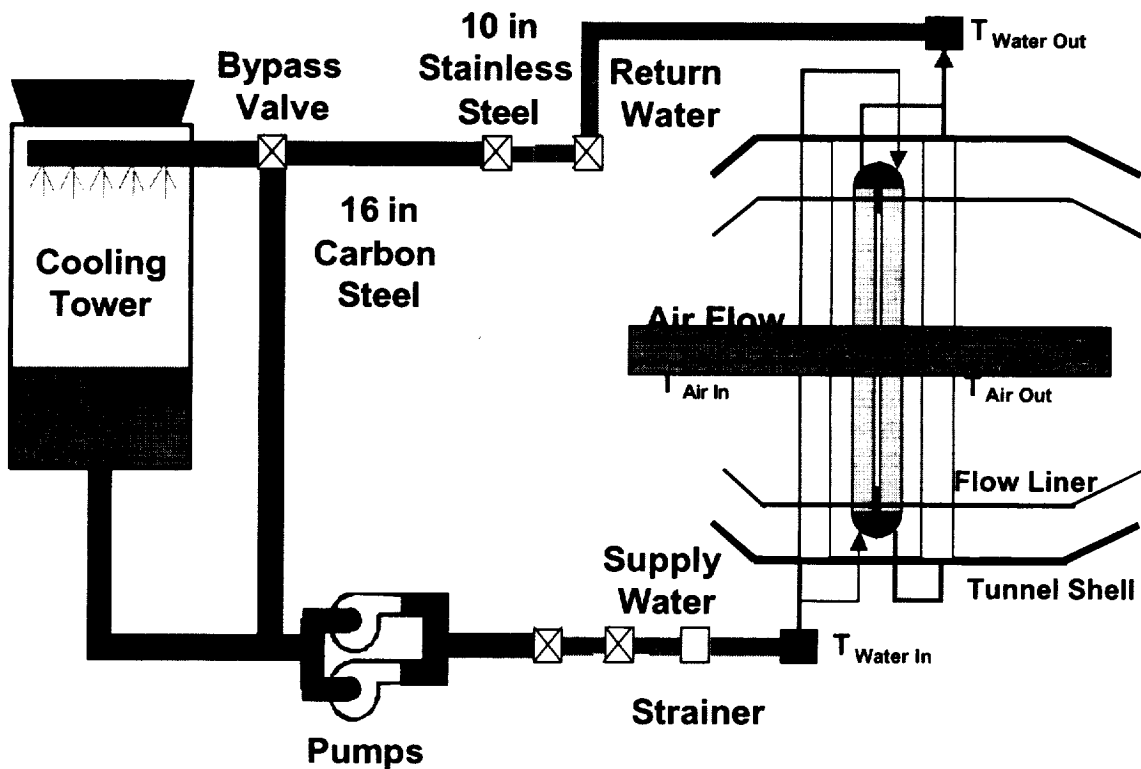


Figure 4 - Cooling Coil Piping Schematic

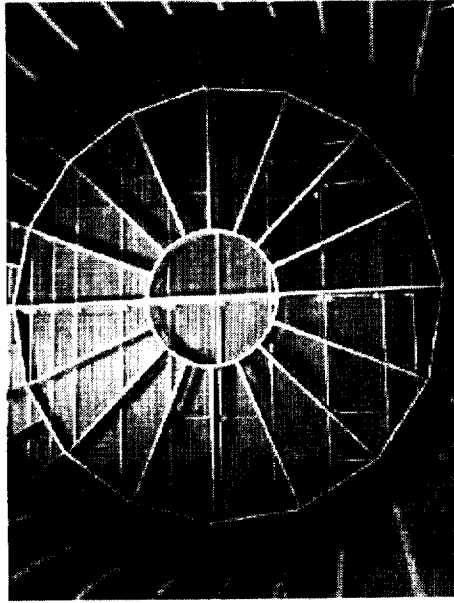


Figure 5 - Upstream Face of Cooling Coil

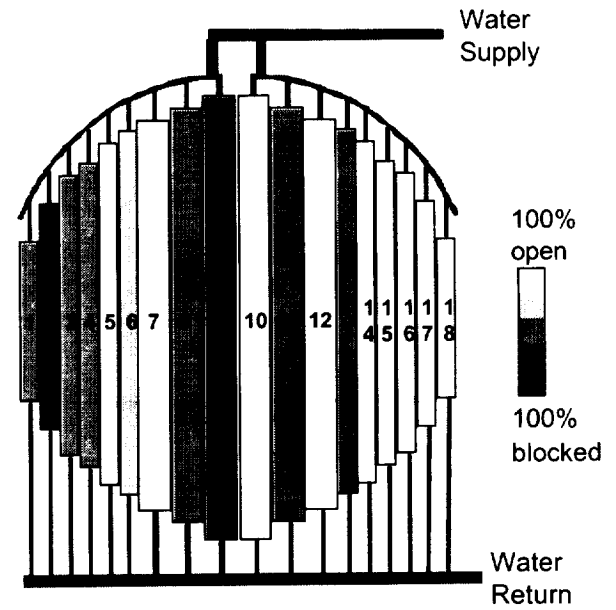


Figure 8 - Flow Blockage of Cooling Coil Bundles (downstream layer)

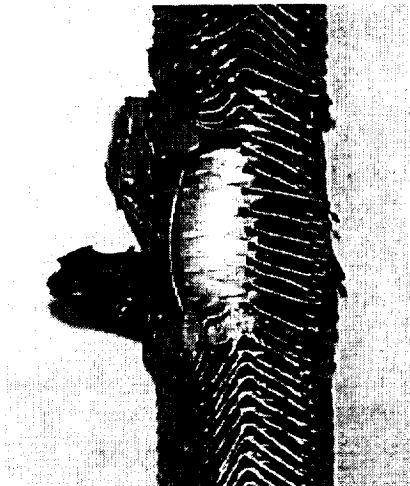


Figure 6 - Ruptured Cooling Coil Tube



Figure 9 - Rust Debris in Strainer

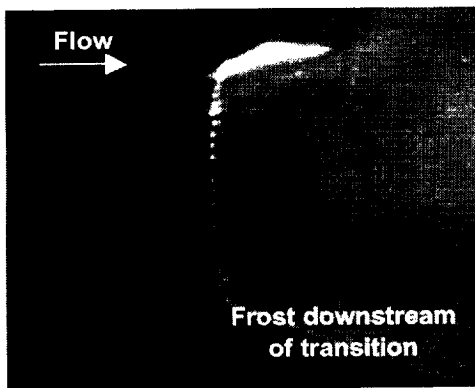


Figure 7 - Frost Contamination on Model Nose

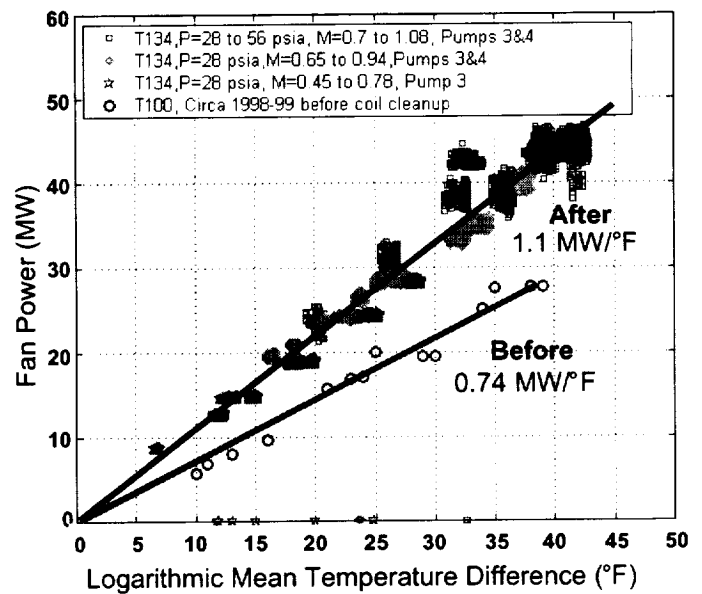


Figure 10 - Cooling Coil Performance

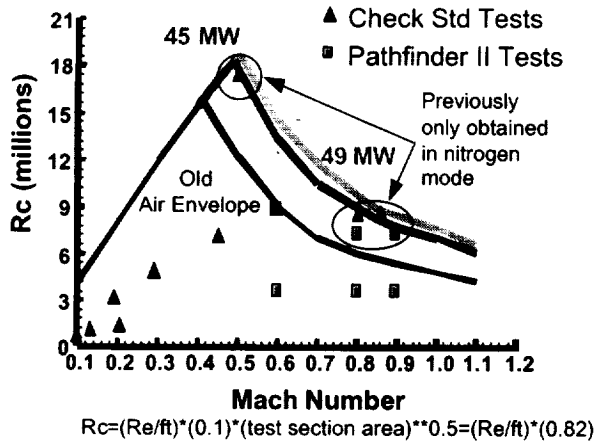


Figure 11 - Additional Test Conditions in Air

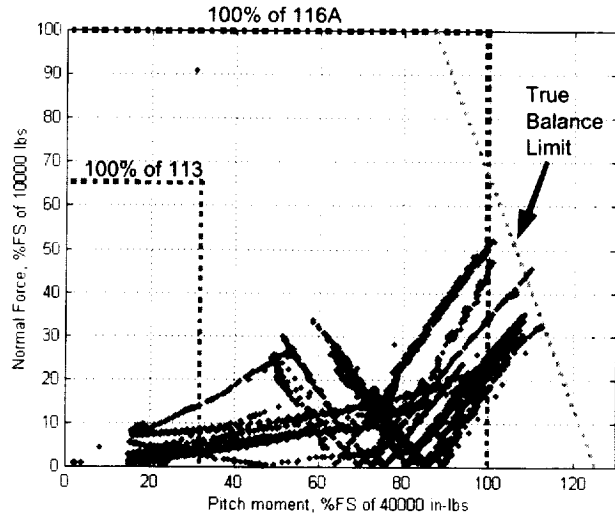


Figure 14 - 113 and 116A Test Load Comparison

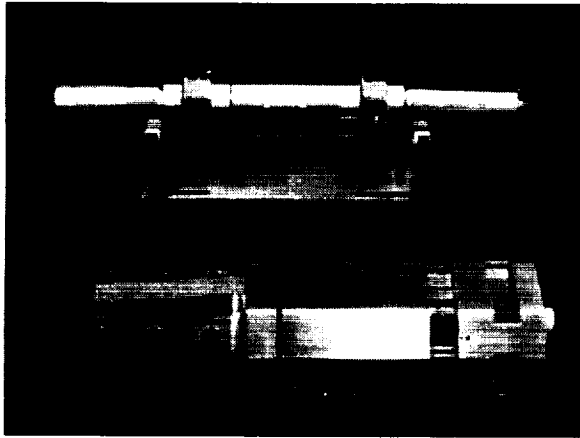


Figure 12 - NTF 113 (top) and 116A (bottom) Balances

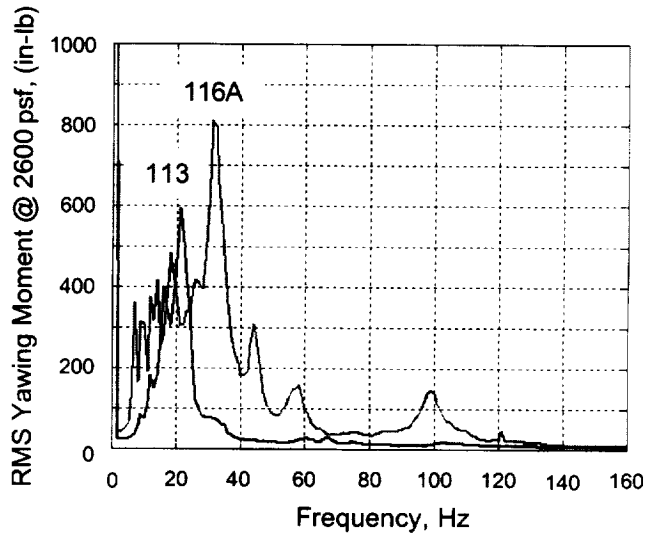


Figure 15 - Model Yaw Dynamics



Figure 13 - New Stiffer Upper Swept Sting

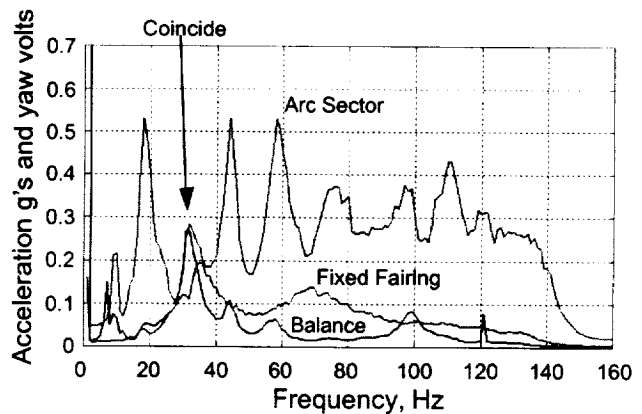


Figure 16 - Structural and Model Modes



